Failure analysis and behaviour of titanium alloy metal matrix composite bolted joints

Som R. Soni* and Hakan Kilic

AdTech Systems Research, Inc, Beavercreek, OH 45432, USA
E-mail: srsoni@adtechsystems.com
*Corresponding author

Michael Camden, Mark M. Derriso and Scott Cunningham

AFRL/VASM, Wright-Patterson Air Force Base, Dayton, OH 45433, USA

Abstract: Pin-loaded hole coupons with tapered geometry were tested to examine the failure behaviour of titanium alloy metal matrix composite (MMC) bolted joints at room temperature and 650°C. The average failure load at 650°C decreased almost to half of the average failure load at room temperature. Additional tests were also carried out at room temperature to investigate different methods to extend the life of the joint. A polyester film was applied around the hole on one face of the specimen, which consequently changed the failure mode and post-failure response of the specimen. Finite element (FE) analyses were performed to predict the behaviour of titanium MMC bolted joints. Failure loads were predicted by solving a boundary value problem representing a single lap bolted joint. A modified concentric cylinders model (CCM) was employed to predict the effective properties used in the FE and failure analyses. Good agreement was shown between the experimental results and the predictions.

Keywords: bolted joints; failure analysis; metal matrix composites; micromechanics.

Biographical notes: Som R. Soni, PhD, is currently the CEO and Senior Scientist of AdTech Systems Research, Inc. Dr Soni has done in-depth investigations of composite structures optimum performance capabilities. He has numerous research publications on vibrations of plates and shells, stress and strength predictions of composite structures including bolted and bonded joints, delamination and finite element techniques. Dr Soni is the founder of AdTech Systems Research, Inc. and co-founder of the American Society for Composites. He received his PhD and MS degrees in Applied Mathematics from the University of Roorkee, India.

Hakan Kilic, PhD, is a Research Scientist/Engineer with AdTech Systems Research, Inc. He has years of experience in the development of micro/ macro mechanical material models used in nonlinear analysis of composite structures; damage modelling and experimental investigation of composite materials and structures. He earned his BS and MS degrees in Civil Engineering at the Middle East Technical University, Turkey. He received his PhD degree from the School of Civil and Environmental Engineering at the Georgia Institute of Technology.

Michael Camden is currently the Deputy Division Chief in the Air Force Research Laboratory's, Air Vehicles Directorate, Structures Division. He has over 25 years experience in structures work including combined thermal/acoustic experimental work. He has received degrees from the following schools: MS, Mechanical Engineering, University of Dayton, 1985; BS, Systems Engineering, Wright State University, 1982; and BS, Technology, Bowling Green State University, 1979.

Mark M. Derriso is a Program Manager in the Advanced Structural Concept Branch of the Air Vehicles Structures Division at WPAFB. He has experience in health monitoring of aircraft structural sustainment, unmanned aero vehicles, and space vehicles; development of unique data acquisition and control systems for testing aircraft structures and materials. He performed research on metal matrix and ceramic matrix composites for the National Aerospace Plane programme. He has a degree in Electronics Engineering Technology from Kentucky State University and an Electrical Engineering degree from Wright State University.

Scott Cunningham is an MS Student in the Department of Aeronautics and Astronautics, Graduate School of Engineering and Management, Air Force Institute of Technology (AFIT), WPAFB, Ohio, USA. Prior to joining AFIT, he worked as a Research Engineer in the Structures Division at the Air Vehicle Directorate of the Air Force Research Laboratory, WPAFB.

1   Introduction

Titanium alloy metal matrix composites (MMCs) are potential materials in the aerospace industry due to their high strength/stiffness-to-density ratios at high temperatures. National Aero Space Plane (NASP) and Integrated High Performance Turbine Engine Technology (IHPTET) programmes have developed a wealth of data in the understanding, characterisation, and life prediction of MMCs. The present work is a part of the in-house research effort of the Air Force Research Laboratory/ Air Vehicles Directorate, Structures Division, Analytical Mechanics Branch (AFRL/ VASM) to investigate the performance of titanium alloy MMC for propulsion and airframe systems.

Numerous experimental, analytical, and numerical investigations have been conducted to characterise the properties and behaviour of titanium alloy MMCs at elevated temperatures. Sun *et al.* [1] performed an experimental study using off-axis coupon specimens to investigate the mechanical behaviour of SCS-6/Ti-6-4 MMC at elevated temperatures. Unidirectional laminates were tested under axial and off-axis

tensile loading at room temperature, 204 and 316°C. It was observed that the Young's modulus remained almost the same at all temperatures for all orientations; however, ultimate strength and yield stress decreased with the increased temperature. Micro/macromechanical material models were also used. For the macromodels, a one-parameter plasticity model was used to predict the nonlinear material behaviour. Fibre/matrix bond strength was estimated assuming elastic fibre and elastic–plastic matrix as constituents in the micromodelling. The strength of the bond between the fibre and the matrix was shown to be weak in the composite by Johnson *et al.* [2]. Rattray and Mall [3] carried out an experimental study using MMC specimens with a central hole or a straight notch. The MMC systems had a quasi-isotropic lay-up with SCS-6 fibre and Timet21S matrix constituents. The tests were performed under tensile loading at room temperature and 650°C. Debonding of fibres was observed as the first failure mode. Failure of fibres and then the matrix failure were observed as the progressive failure modes. Roush and Mall [4] conducted an experimental study to investigate the fracture behaviour of SCS-9/Timet21s MMC at elevated temperatures. Unidirectional, cross-ply, and quasi-isotropic specimens with holes and pin-joints were tested under tensile load at 0, 482, and 650°C. Off-axis ply interfacial failures were observed as the first damage mechanism in the cross-ply and quasi-isotropic laminates at all temperatures. Debonding and failure of the 0°C fibres with matrix plasticity were the progressive failure mechanisms at 0 and 482°C. Additionally, matrix cracking was also observed in the cross-ply and quasi-isotropic laminates at 650°C. Fibre debonding and fibre cracking were the failure mechanisms of unidirectional specimens at all temperatures. Matrix cracking and matrix plasticity were also observed at 0 and 482, and 650°C, respectively.

Santhosh *et al.* [5] considered damage in the form of fibre–matrix debonding and they employed a nonlinear finite element analysis procedure to predict directional stress–strain response of the composite. Jansson and Kedward [6] investigated the effects of weak fibre–matrix interface on the effective properties of SCS-6/Ti-15-3 MMC. They found the transverse tensile and shear moduli are reduced significantly due to the relation of the residual compressive stresses at the fibre–matrix interface. Aghdam *et al.* [7] and Bednarcyk and Arnold [8] used finite element models along with micromechanics-based models for the prediction of longitudinal stress–strain response and failure of SiC/Ti MMCs. In the former study, the effects of residual stress and the weak interface were included in the proposed models. The micromodel proposed in the latter study takes into account the longitudinal fibre breakage. Majumdar and Newaz [9] characterised the mechanical response of SCS-6/Ti-15-3 MMC at room temperature and 539°C. Four different laminates, $[0]_8$, $[90]_8$, $[0/90]_{2s}$, and $[\pm 45]_{2s}$, were tested under tension. It was observed that regardless of the lay-up configuration, mechanical properties decreased at elevated temperatures due to matrix flow stress and fibre/matrix debonding. Aboudi *et al.* [10] used the method of cells to predict the temperature dependent response of MMC laminates.

Since most structural components are subject to multi-axial stress states, one of the important issues is the performance of MMC materials and components with loaded fastener holes and cutouts. These holes, cutouts are stress concentration areas and may have a crucial influence over the material response, structural mode, and magnitude of failure. Therefore, more research still needs to be done on

the Ti-alloy MMCs in order to completely characterise the material behaviour and analyse the structural components at elevated temperatures and under different types of loading conditions.

To this end, a combined experimental, analytical, and numerical study has been performed in this study to investigate the behaviour of SCS-6/Ti-15-3 MMC bolted joints. In the first part, pin-loaded hole coupons with tapered geometry were tested under tension to examine the failure behaviour of the joint at room temperature and 650°C. Additional tests were carried out at room temperature to investigate the application and validity of different methods to extend the life of the joint. Thus, a polyester film was applied around the hole on one face of the specimen. In the second part of this study, a modified concentric cylinders model (CCM) along with the classical lamination theory (CLT) is employed to predict the ply and laminate properties used in the finite element (FE) and failure analyses. FE analyses are performed to predict the behaviour of titanium MMC bolted joints and compare the results with the experimental data. Failure load predictions are carried out using a previously developed code for the failure analysis of bonded and bolted composite joints.
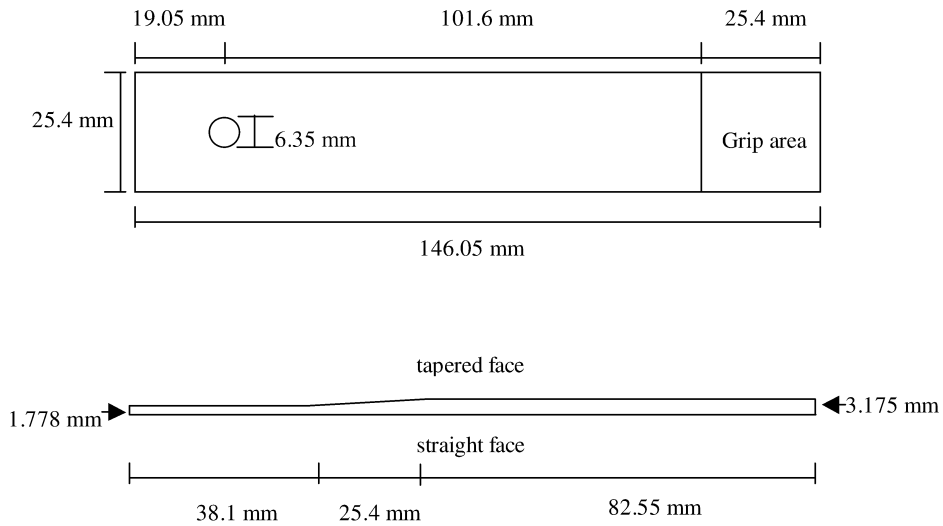
2   Test specimen preparation

The MMC material investigated in this study has titanium Ti-15-3 alloy as the matrix and silicon carbide SCS-6 as the fibre constituents. The laminate has a quasi-isotropic lay-up of $[0/+45/-45/90]_s$ with 33% fibre volume fraction. Table 1 gives the constituent matrix and fibre properties at different temperatures. The tested coupons have a tapered geometry that introduces a bending effect in addition to the axial bolt load (Figure 1).

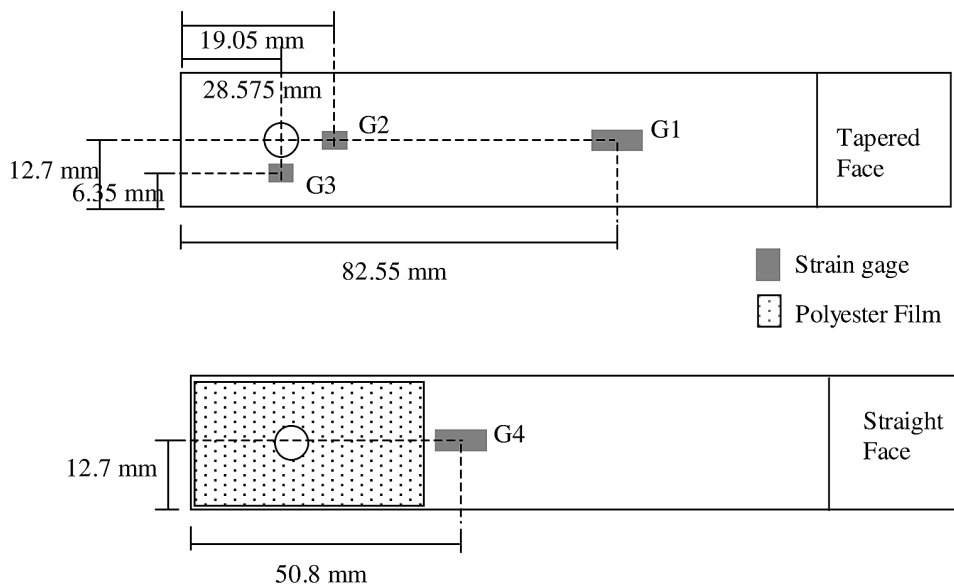**Table 1**   Constituent material properties fibre (f) and matrix (m)

Temperature (°C)	E_f (GPa)	ν_f	E_m (GPa)	ν_m
25	393	0.25	86.3	0.36
482	376	0.25	72.2	0.36
538	374	0.25	77.8	0.36
566	373	0.25	64.4	0.36
650	370	0.25	53	0.36

Figure 1 Test specimen geometry

19.05 mm   101.6 mm   25.4 mm

25.4 mm

6.35 mm

Grip area

146.05 mm

tapered face

1.778 mm   3.175 mm

straight face

38.1 mm   25.4 mm   82.55 mm

For the experiments at room temperature, two specimens (S1 and S2) were tested without strain gages while four strain gages were applied to specimen (S3). The locations of the strain gages are shown in Figure 2. Another set of three specimens was tested to examine the effects of polyester film on the behaviour of the MMC joint. An extensometer was attached to the specimens tested at 650°C (S7 and S8); no strain gages or polyester film were applied on the specimens. These specimens were tested in a furnace specifically made for heating the specimens uniformly.

Figure 2 Strain gage and polyester film locations

19.05 mm

28.575 mm

G2   G1

12.7 mm

6.35 mm   G3

Tapered
Face

82.55 mm

■ Strain gage

▦ Polyester Film

G4

12.7 mm

Straight
Face

50.8 mm

The polyester film applied on the specimens is a real-time pressure sensitive film to observe the pressure loads between any two contacting surfaces. In this study, it is not used for measuring pressure, but is introduced as a material to increase the strain capacity of the MMC joints due to its significantly high ultimate strain characteristic. The film is made from polyethylene terephthalate (PET). Although its contribution to the stiffness of MMC material is very small, its ultimate strain goes far beyond the 20% reported in the literature [11].

The polyester film was applied on the straight face of the specimens, as shown in Figure 2, because this face is under additional tensile strain due to the bending of the specimen with tapered geometry. Three different application methods for the polyester film were employed. For two of the specimens, the film was put on the surface using commercially available super-glue. Specimen S4 was tested after 16 h and the specimen S5 after 4 h of glue-hardening time. In the case of specimen S6, a special strain-gage adhesive was applied and tested after 4 h of cure time. Three strain gages were used on the tapered side of specimen S4, as seen in Figure 2. Table 2 summarises the tests performed and the specimens used.
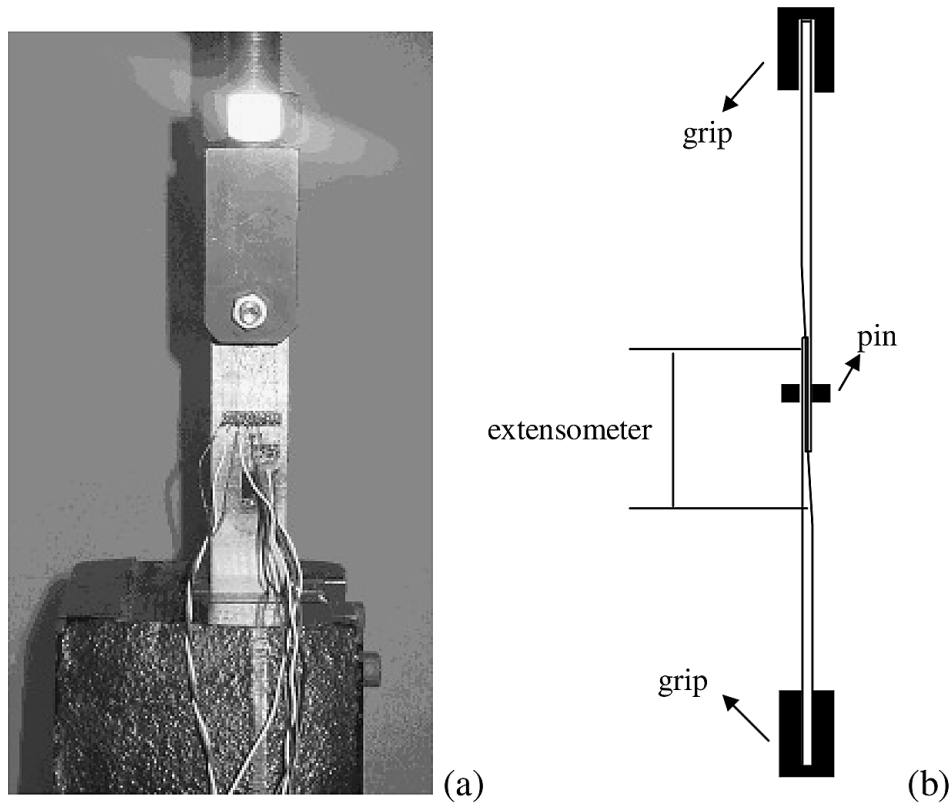
Table 2   Summary of tests performed and test specimens

Test no.	No. of strain gages	Extensometer	Temperature	PET film	Adhesive type	Cure time (h)
S1	n/a	no	room	no	n/a	n/a
S2	n/a	no	room	no	n/a	n/a
S3	4	no	room	no	n/a	n/a
S4	3	no	room	yes	Glue 1	16
S5	3	no	room	yes	Glue 1	4
S6	n/a	no	room	yes	Glue 2	4
S7	n/a	yes	650°C	no	n/a	n/a
S8	n/a	yes	650°C	no	n/a	n/a

Note: n/a – not applicable

3   Experimental study

All the specimens tested at room temperature were placed in a 20-kips ATS test machine. The thicker side of the specimen was clamped using mechanical grips while the pin load was applied at the hole of the specimen as seen in Figure 3a. Tests were run under displacement control with a loading rate of 0.02 in/min. In the case of the tests at 650°C, two specimens were bolted together using a pin and gripped at both ends as seen in Figure 3b.

Figure 3 Test set-up (a) at room temperature and (b) at 650°C

(a) (b)

The load–stroke responses of all specimens tested at room temperature are plotted in Figure 4. The experimental results show that there is no effect of the polyester film on the initial response of MMC joint. However, as seen in Figure 4, the responses of specimens with and without the PET film are different at and after the ultimate load. The average ultimate load for the specimens without the PET film (S1 to S3) is 24.15 kN. The average first failure load is 11% lower (21.53 kN) for the specimens (S4 to S6) with the PET film. In the case of the specimens S1 to S3, failure is brittle and occurs just after the ultimate stress point. The mode of failure is net-tension as seen in Figure 5. Application of the PET film has provided the redistribution of stresses in the material around the bolt hole area and the material did not fail in tension.

Figure 4   Load stroke readings for all specimens tested at room temperature
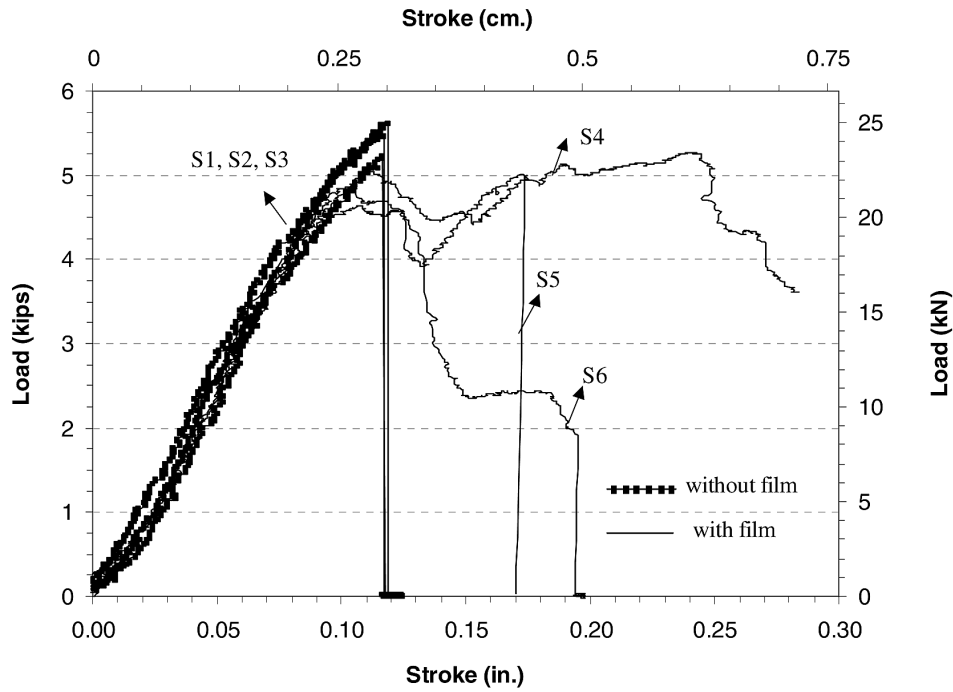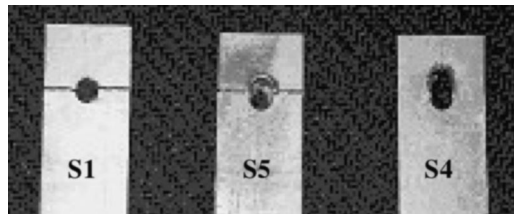

Figure 5   Failed specimens with and without PET polyester film at room temperature

In the case of the specimens with PET film, the mode of first failure is bearing type. Application of the polyester film changed the failure mode of the tested MMC joints. Although it did not increase the load capacity of the joints, it has extended the life of the tested MMC joints when the significant increase in their strain capacity is considered. In specimens S5 and S6, the progressive failure mode is net-tension where there is no change in the failure mode of the specimen S4 (Figure 5). However, there is a second peak load for the specimens S4 and S5, which is higher than the first failure load. Differences in the progressive failure behaviours of the joints with PET film (S4 to S6) can be attributed to the type of adhesives used between the film and the specimen surface, and the adhesive hardening time.

The average failure load obtained from the two tests performed at 650°C is 11.70 kN, which is almost 50% of the average ultimate load obtained from the tests at room temperature. The failure mode is net-tension.

4 Concentric cylinders model (CCM)

Research on Ti-alloy MMCs [1–9,12,13] showed the fibre/matrix interface is very important due to the significant difference between the thermal expansion coefficients of the SCS fibres and Ti-alloy matrix. The matrix has a larger coefficient of thermal expansion; therefore, large compressive radial stresses occur at the interface between the matrix and the fibre as the composite is cooled from the processing temperature. Hence, the predicted effective material properties via micromodels without considering this weak fibre/matrix interface can be unconservative.

In this study, a previously developed software code, ASCA [14], is used to predict the effective elastic material properties of the SCS-6/Ti-15-3 MMC. This code uses the concentric cylinders micromodel developed by Pagano and Tandon [15,16]. Following the study done by Subramanian *et al.* [13], the CCM in this study consists of six layers to take into account the effects of weak fibre/matrix interface in MMCs. as seen in Figure 6. The four layers between the fibre and matrix layers are considered as the interphase layers. The radii of fibre and matrix layers are calculated using a fibre volume fraction of 33%. The matrix radius (r_m) is taken as 5.080 mm and the fibre radius (r_f) is calculated as 2.921 mm. The radii of fibre (r_f), matrix (r_m), and interphase (r_{i1}, r_{i2}, r_{i3}, r_{i4}) layers are tabulated in Table 3.

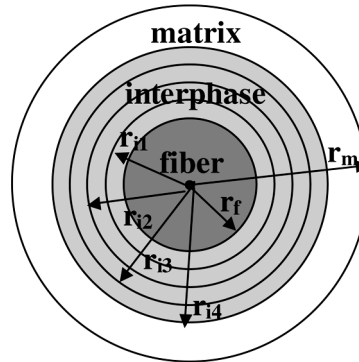**Figure 6** Concentric cylinders micromechanical model

Table 3 Radii and properties of layers used in the concentric cylinders model

	Radius (mm)	Young's modulus (GPa)		Modulus after yield (GPa)		Poisson's ratio	
		room	*650°C*	*room*	*650°C*	*room*	*650°C*
Fibre	2.921	393.00	370.00	393.00	370.00	0.25	0.25
Matrix	5.080	86.30	53.00	13.00	0.25	0.36	0.36
Interphase 1	3.124	13.79	6.89	2.08	0.03	0.30	0.30
Interphase 2	3.302	27.58	13.79	4.15	0.07	0.30	0.30
Interphase 3	3.480	41.37	27.48	4.23	0.13	0.30	0.30
Interphase 4	3.658	55.16	41.37	8.31	0.20	0.30	0.30

The interphase region is divided into four layers of equal thickness. The total thickness and the moduli of the interphase layers are calibrated. Matrix and interphase constituents are taken as isotropic bilinear materials and their corresponding elastic properties at room temperature and 650°C are reported in Table 3. Fibres are considered as linear, elastic, and transversely isotropic. During the calibration, an attempt is made to match the overall measured (experimentally obtained) longitudinal Young's modulus (in the fibre direction) of unidirectional SCS-6/Ti-15-3 MMC material by changing the elastic properties and the total thickness of the interphase layers. The experimentally obtained value of longitudinal Young's modulus was reported as 178.7 GPa in Santhosh *et al.* [5].
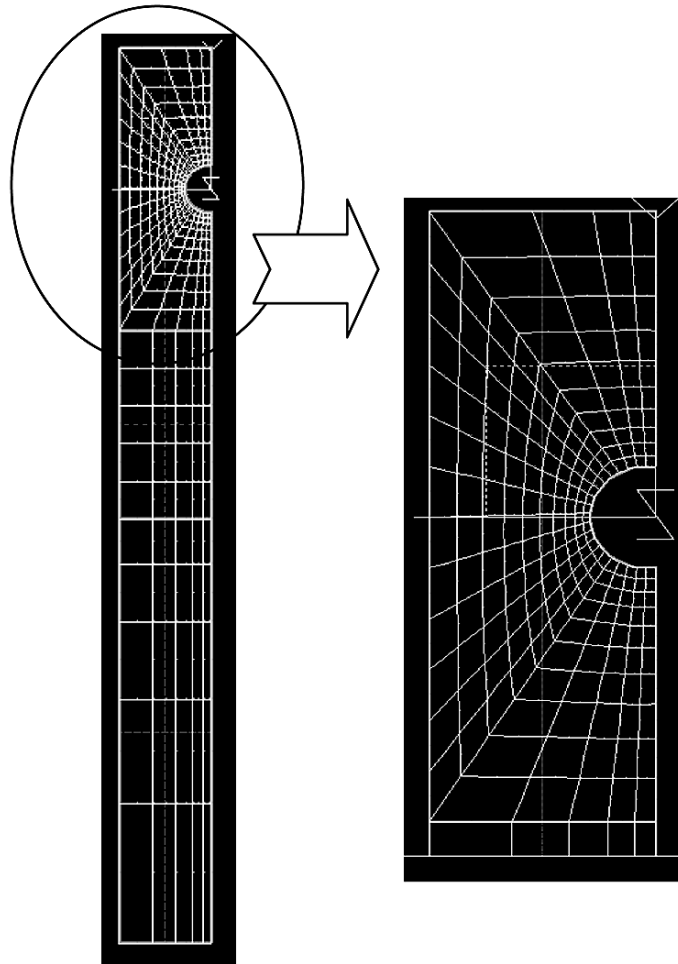
The predicted in-plane effective elastic properties of the SCS-6/Ti-15-3 MMC material at room temperature and 650°C for unidirectional fibre-reinforced composite and for the quasi-isotropic lay-up of $[0/+45/-45/90]_s$ are given in Table 4.

Table 4   Predicted effective elastic properties of SCS-6/Ti-15-3 MMC

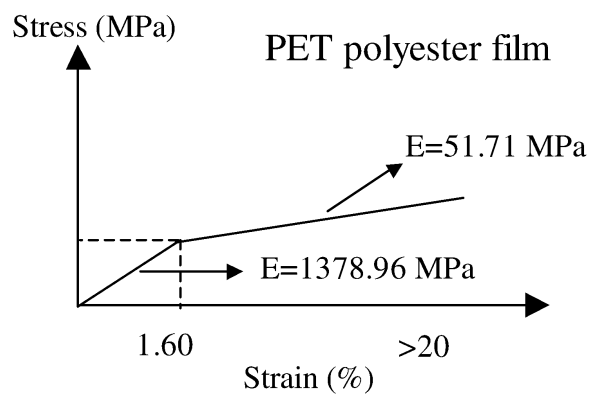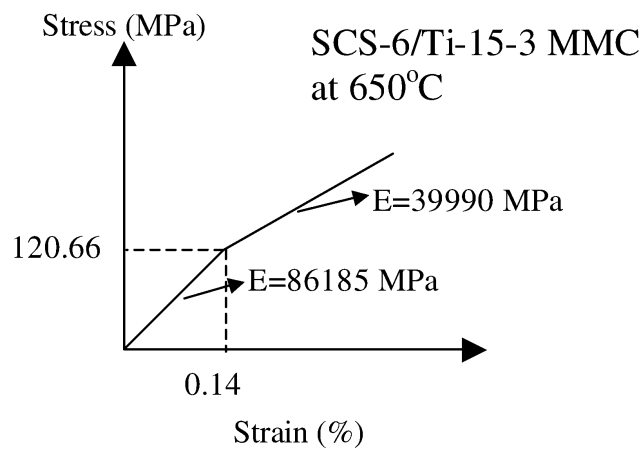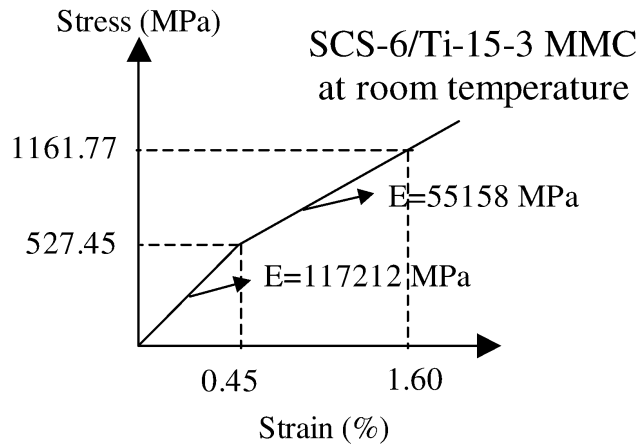|	*Room temperature*				*650°C*			
	E_{11} *(Gpa)*	E_{22} *(GPa)*	G_{12} *(GPa)*	ν_{12}	E_{11} *(GPa)*	E_{22} *(GPa)*	G_{12} *(GPa)*	ν_{12}
Unidirectional	178.0	90.8	33.4	0.32	152.4	56.1	20.3	0.32
$[0/+45/-45/90]_s$	117.2	117.2	44.7	0.32	86.2	86.2	32.7	0.32
Predicted material properties after yielding								
Unidirectional	137.2	15.8	5.6	0.32	122.0	0.25	0.09	0.32
$[0/+45/-45/90]_s$	55.2	55.2	20.9	0.32	40.0	40.0	15.2	0.32

5   Finite element (FE) analysis

FE models are used to simulate the tests with pin-loaded specimens. Due to symmetry considerations, half of the plate is modelled in the FE analysis as seen in Figure 7. After performing a convergence study, the model consists of 220 3D 20-node brick elements. One element is used through the thickness; however, using quadratic solid elements enables to capture the bending effects due to the tapered geometry of the specimen. The pin is modelled with rigid elements. Contact is explicitly modelled between the pin and the specimen.

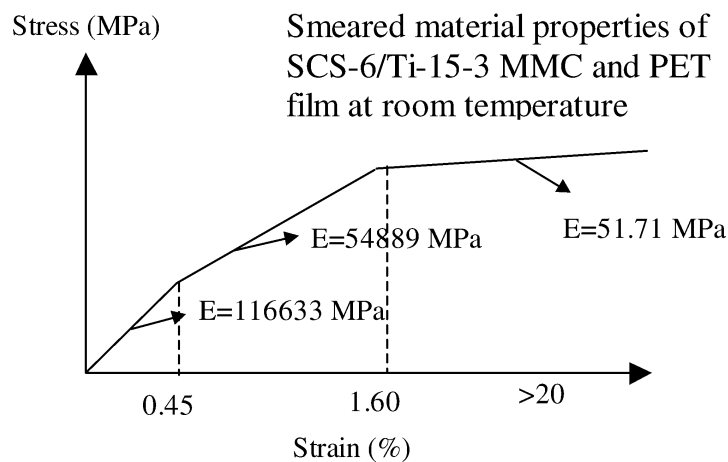**Figure 7** FE model of a pin-loaded MMC joint

Isotropic bilinear material models are used to represent the material behaviours of SCS-6/Ti-15-3 MMC and PET polyester film, as shown in Figure 8. The PET material model is approximated based on the material properties available in the literature and from the manufacturer [11,17]. The Poisson's ratios for MMC and PET materials are taken as 0.32 and 0.44, respectively. The effective material properties for the quasi-isotropic MMC material predicted using the micromechanical material model (Table 4) are used in the bilinear material models for the MMC at room temperature and 650°C. Since the proposed micromodel is not capable of predicting the failure stresses and strains of MMC material, experimental results in Santhosh *et al*. [5] are used to determine the ultimate stress value of the MMC material at room temperature. The ultimate strain is calculated using the predicted elastic moduli. The adhesive between the PET film and the specimen is not modelled explicitly in the FE analysis.

Figure 8   Material models for MMC and PET film materials

Stress (MPa)

SCS-6/Ti-15-3 MMC
at room temperature

1161.77

E=55158 MPa

527.45

E=117212 MPa

0.45   1.60

Strain (%)

Stress (MPa)

SCS-6/Ti-15-3 MMC
at 650°C

E=39990 MPa

120.66

E=86185 MPa

0.14

Strain (%)

Stress (MPa)

PET polyester film

E=51.71 MPa

E=1378.96 MPa

1.60   >20

Strain (%)

For the analysis of specimens without the PET film, the initial and degraded modulus values of the MMC material model are used for all the elements in the model. In the case of the analysis of specimens with the PET film, the film is not modelled explicitly; instead, smeared material properties are used for the elements in the polyester film area. The initial and degraded modulus values of the MMC material model are used for the other elements of the FE model. Figure 9 shows the material model used for the finite elements in the area where the PET film is applied. The ratio of the specimen thickness to the PET film thickness is considerably low and is taken as 1/200 in calculating the smeared material properties of the elements. Using this thickness ratio, weighted average moduli are calculated as 116,633 and 54,889 MPa for the initial modulus and the modulus after yielding, respectively. Only the PET degraded modulus, 51.71 MPa is used for the elements whose average strain goes beyond 1.60%, after which the elastic modulus of MMC material is no longer used in the calculations for the FE analysis of joints with PET film.

Figure 9   Material model for the elements in the PET film area, at room temperature

Figures 10 and 11 show the load–stroke responses from the models and the experimental results at room temperature. The FE predictions are in good agreement with the test results of the specimens with and without the polyester film. Predicted FE results are also compared with the experimental strain data at room temperature and plotted as four curves in the form of remote stress versus the strains measured from the four strain gages on the specimens, as shown in Figure 12. The last point in each experimental curve corresponds to the ultimate or first failure load of the specimen at room temperature. The FE models predict the behaviour of MMC joints in good agreement with the experimental results, even in the high stress concentration region due to the circular hole.

Figure 10 Load–stroke curves for the specimens without PET film at room temperature
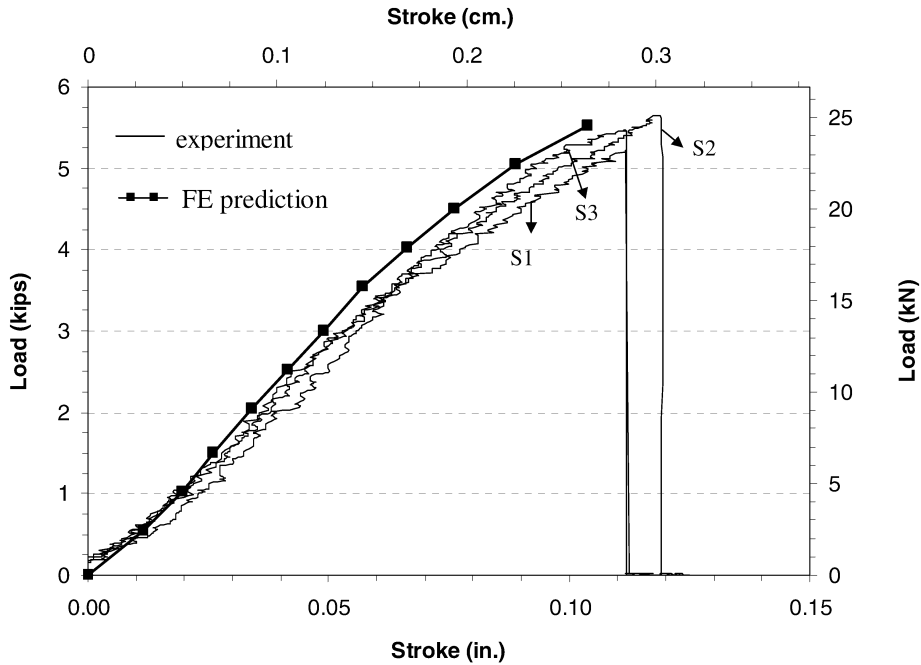

Figure 11 Load–stroke curves for the specimens with PET film at room temperature
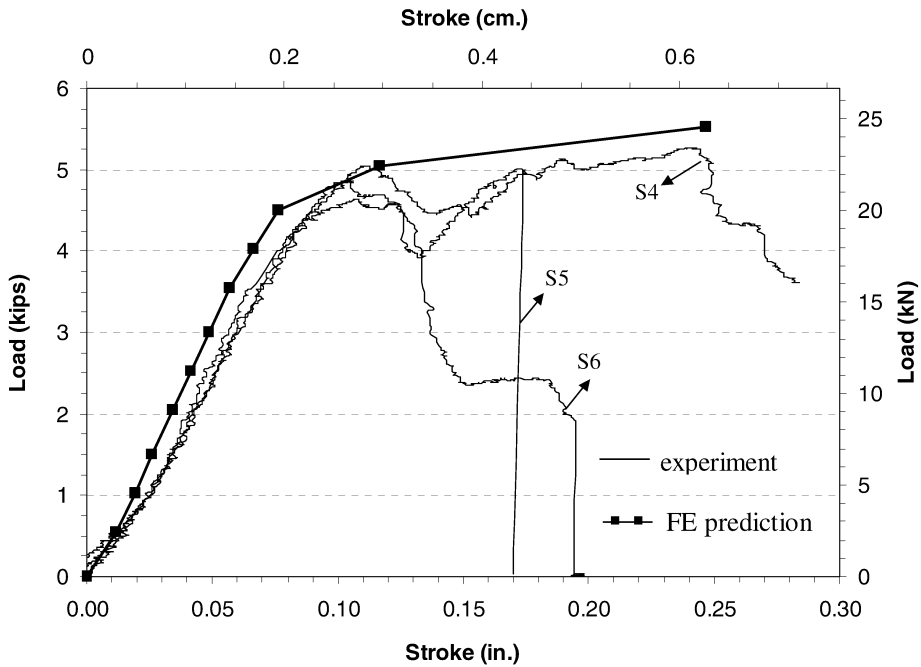
Figure 12 Stress–strain plots for different locations of strain gages at room temperature
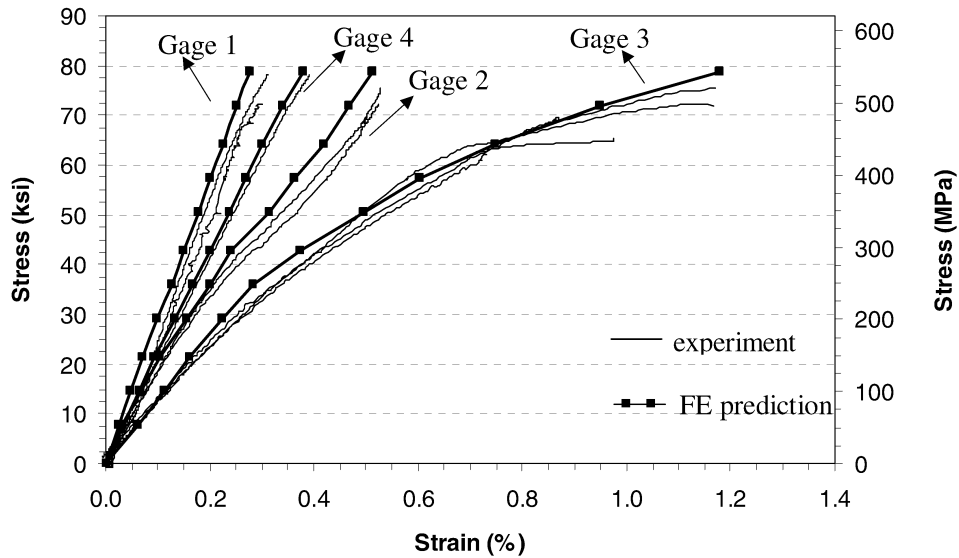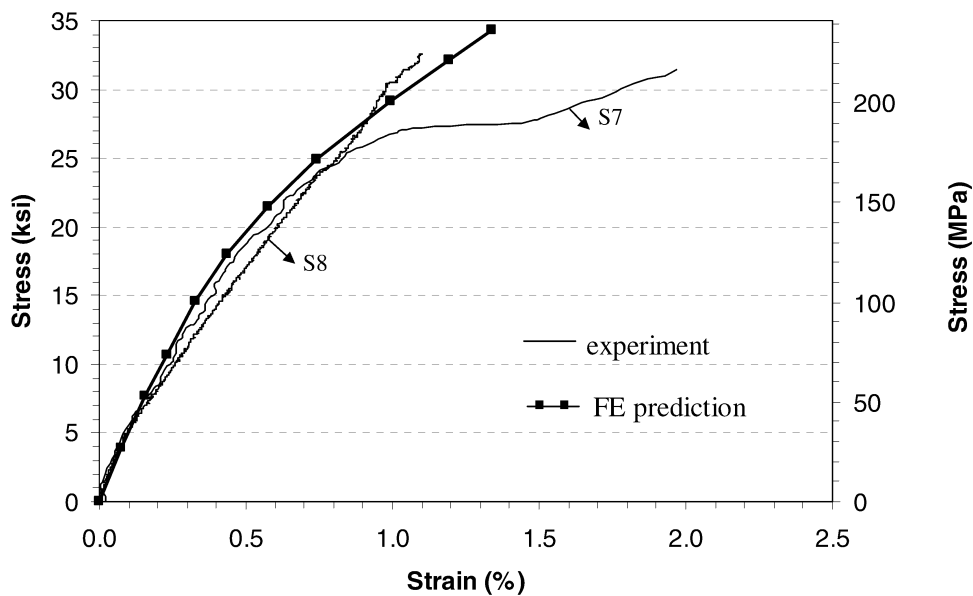

Figure 13 shows the FE analysis and the experimental results of two tests at 650°C. The experimental curves are plotted with applied remote stress versus strain calculated from the displacement readings of extensometer. The extensometer has a gage length of 6.35 cm; it was placed on the specimen as shown in Figure 3. The overall prediction of the model is good, especially in the low strain range.

Figure 13 Remote stress versus extensometer strain curves for the specimens at 650°C
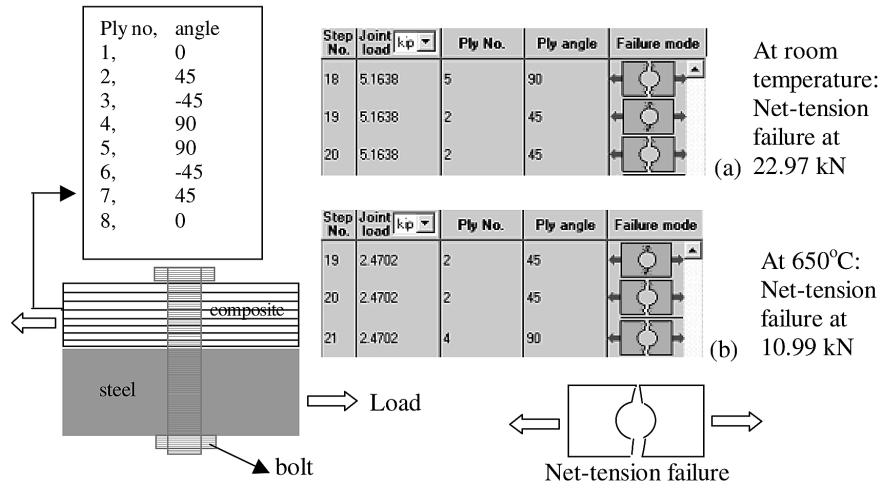
6   Failure analysis of MMC bolted joints

In Section 6, stress–strain and load–stroke responses of the MMC bolted joints are predicted using FE analysis. However, failure load and the mode of failure cannot be predicted using the FE techniques employed in the current study. Hence, a previously developed computer code for the failure analysis of bonded and bolted composite joints, BBJ [18], is used to predict the failure load and the failure mode of MMC joints. Failure load predictions of specimens without the PET film at room temperature and 650°C are carried out solving a boundary value problem representing a single lap bolted joint. In this code, a two-dimensional laminate analysis and the finite difference fastener analysis are incorporated into a progressive failure analysis of bonded and bolted joints. The foundation of this work can be found in References [19–21].

The two-dimensional laminate analysis is based on the Lekhnitskii's [22] complex variable solution. The two-dimensional stress field is expressed in Airy stress functions to identically satisfy the equilibrium equations for every point in the plate domain. Using the constitutive material law and compatibility equations, the solution to the plate problem is obtained in terms of coefficients of complex functions in Laurent series. Using the boundary conditions, the values of the coefficients are determined. The solution procedure is explained in details in Ramkumar *et al.* [20]. The fastener analysis takes into account the bending and shear deformation effects on the fastener flexibility. The stress field at the fastener location is computed modelling the fastener as a beam on an elastic foundation. The elastic foundation is represented by uniform moduli of plies in the bolted laminate. Bilinear elastic material behaviour is used for each ply to take into account for stiffness degradation after initial failure. This method allows a progressive failure analysis. Different failure criteria can be used for the failure analysis procedure. In the current study, the average stress criterion is used to predict the failure load of the MMC bolted joints. The failure criterion predicts three different modes of failure; net-section, bearing, and shear-out. This failure analysis code has been verified for different types of composite materials, including various classes of MMCs [19–21].

The MMC material behaviours, shown in Figure 8, are used for the failure analysis of bolted joints at room temperature and 650°C. A composite plate with eight layers, bolted to a steel plate, is used to model a single-lap bolted joint, as seen Figure 14. An axial tensile load is applied to the joint.

Figure 14 shows the loads and the modes of failure of composite laminate pertaining to the room temperature conditions and at elevated temperature of 650°C. The results are tabulated in five columns. The first column shows the step number, which is also the increment number for an incremental solution under an applied load. The failure load value is shown in column two. The number and orientation of the ply in which failure has occurred at the increment are shown in columns three and four, respectively. The last column shows whether the failure mode is net-section, bearing, or shear-out. The predicted ultimate failure loads are 5% higher and 8% lower than the experimentally obtained average values for the specimens at room temperature and 650°C, respectively. The predicted mode of failure is net-tension, which is same as the experimentally observed mode.

Figure 14 Failure load and mode predictions at (a) room temperature and (b) 650°C

7   Conclusions

A combined experimental, analytical, and numerical study is presented to understand the failure mechanism and behaviour of SCS-6/Ti-15-3 MMC joints at room temperature and 650°C. A polyester film was applied on the specimens to examine its effects on the failure mode and load at room temperature. The preliminary test results show the polyester film extends the life of the joint as the failure mode changes from net-tension to bearing type. FE models are employed to simulate and predict the response of the MMC joints with and without the polyester film. Failure load predictions are made by solving a boundary value problem representing a single lap bolted joint. A modified CCM is employed to predict the effective properties used in the failure and FE analyses. Good agreement is shown when comparing the experimental results and the predictions.

Acknowledgement

References

1 Sun, C.T., Chen, J.L., Sha, G.T. and Koop, W.E. (1993) 'An investigation of the mechanical behavior of SCS-6/Ti-6-4 metal matrix composite at elevated temperatures', *Composites Science and Technology*, Vol. 49, pp.183–190.

2 Johnson, W.S., Lubowinski, S.J. and Highsmith, A.L. (1990) 'Mechanical characterization of unnotched SCS-6/Ti-15-3 metal matrix composites at room temperature' in J.M. Kennedy, H.H. Moeller and W.S. Johnson (Eds.) *Thermal and Mechanical Behavior of Metal Matrix and Ceramic Matrix Composites, ASTM STP 1080*, Philadelphia, PA: American Society of Testing and Materials, pp.193–218.

3   Rattray, J. and Mall, S. (1994) 'Tensile fracture behavior of notched fiber reinforced titanium metal matrix composite', *Composite Structures*, Vol. 28, pp.471–479.

4   Roush, J.T. and Mall, S. (1994) 'Fracture behavior of a fiber-reinforced titanium matrix composite with open and filled holes at room and elevated temperatures', *J. Composites Technology and Research*, Vol. 16, No. 3, pp.201–213.

5   Santhosh, U., Ahmad, J. and Nagar, A. (1992) 'Non-linear micromechanics analysis prediction of the behavior of titanium-alloy matrix composites', *Fracture and Damage*, Vol. 27, pp.65–76.

6   Jansson, S. and Kedward, K. (1997) 'Design considerations and mechanical properties of SCS6/Ti 15-3 metal matrix composite after debond', *Composite Structures*, Vol. 39, pp.11–19.

7   Aghdam, M.M., Smith, D.J. and Pavier, M.J. (2000) 'Finite element micromechanical modeling of yield and collapse behavior of metal matrix composites', *J. the Mechanics and Physics of Solids*, Vol. 48, pp.499–528.

8   Bednarcyk, B.A. and Arnold, S.M. (2001) 'Micromechanics-based deformation and failure prediction for longitudinally reinforced titanium composites', *Composites Science and Technology*, Vol. 61, pp.705–729.

9   Majumdar, B.S. and Newaz, G.M. (1994) 'A comparison of mechanical response of MMC at room and elevated temperatures', *Composites Science and Technology*, Vol. 50, pp.85–90.

10 Aboudi, J., Mirzadeh, F. and Herakovich, C.T. (1994) 'Response of metal matrix laminates with temperature-dependent properties', *J. Composites Technology and Research*, Vol. 16, No. 1, pp.68–76.

11 Lam, S.W., Xue, P., Tao, X.M. and Yu, T.X. (2003) 'Multi-scale study of tensile properties and large deformation mechanisms of polyethylene terephthalate/ polypropylene knitted composites', *Composites Science and Technology*, Vol. 63, No. 10, pp.1337–1348.

12 Mall, S. and Nicholas, T. (Eds.) (1997) *Titanium Matrix Composites: Mechanical Behavior*, Lancester, PA: Technomic Publishing Co, Inc.

13 Subramanian, S., Foringer, M.A. and Soni, S.R. (1995) 'Prediction of the response of metal matrix composite laminates under multiaxial loading', *Proceedings of the 10th ASC Technical Conference on Composite Materials*, Santa Monica, CA, pp.559–568.

14 ASCA, Automated System for Composite Analysis. Available from: http:// www.adtechsystems.com/asca.html

15 Pagano, N.J. and Tandon, G.P. (1988) 'Elastic response of multi-directional coated-fiber composites', *Composites Science and Technology*, Vol. 31, pp.273–293.

16 Tandon, G.P. (1995) 'Use of composite cylinder model as representative volume element for unidirectional fiber composites', *J. of Composite Materials*, Vol. 29, pp.388–409.

17 Sensor Products Inc. Available from: http://www.sensorprod.com/pressurex.html

18 BBJ, Bolted and Bonded Joint Software. Available from: http://www.adtechsystems.com/ bbj.html

19 Garbo, S.P. and Ogonowski, J.M. (1978) 'Effect of variances and manufacturing tolerances on the design strength and life of mechanically fastened composite joints', *Methodology Development and Data Evaluation*, *AFWAL-TR-81-3041*, Vol. 1, Air Force Wright Aeronautical Laboratories, WPAFB, OH: Flight Dynamics Laboratory.

20 Ramkumar, R.L. *et al.* (1985) 'Strength analysis of composite and metallic plates bolted together by a single fastener', *AFWAL-TR-85-3064*, Air Force Wright Aeronautical Laboratories, WPAFB, OH: Flight Dynamics Laboratory.

21 Rastogi, N., Xie, M. and Soni, S.R. (1997) 'Strength prediction codes for bolted joints in composite structures', *Proceedings of the AIAA/ASME/ASCE/AHS/ASC 38th Structures, Structural Dynamics, and Materials Conference*, Orlando, FL, April 7–10, pp.1088–1098.

22 Lekhnitskii, S.G. (1968) *Anisotropic Plates*, New York: Gordon and Breach Science Publishers.